ACS Energy LETTERS

http://pubs.acs.org/journal/aelccp

PERSPECTIVE

Mesoscale Functional Imaging of Materials for Photovoltaics

Elizabeth M. Tennyson, John M. Howard, and Marina S. Leite*

Department of Materials Science and Engineering, and Institute for Research in Electronics and Applied Physics, University of Maryland, College Park, Maryland 20740, United States

ABSTRACT: **Further global adoption of photovoltaic energy conversion technologies is contingent on sustained progress toward widespread grid-parity. For that, solar cell materials composed of microscale grains and nanoscale boundaries show the highest potential due to their large theoretical efficiency and low-cost fabrication methods. Here we outline the current challenges facing hybrid perovskites and prevalent thin-film polycrystalline materials for photovoltaics. We offer our perspective on how mesoscale functional imaging can enable a complete understanding of the physical and chemical processes restricting their performance, completing the materials science structure−properties−processing−performance tetrahedron. First, we present the key characteristics of hybrid perovskites, CdTe, CIGS, CZTS, and pc-GaAs, emphasizing their main limitations. Second, we discuss how novel imaging methods based on electron and scanning probe microscopies can be realized to provide quantitative information about the relevant parameters (figures-of-merit) that define solar cell performance, with nanoscale spatial resolution. Finally, we offer our vision for the upcoming years, wherein correlative functional microscopy will lead to a complete narrative of the electrical, optical, structural, and chemical properties of these materials, including their surface and bulk properties.**

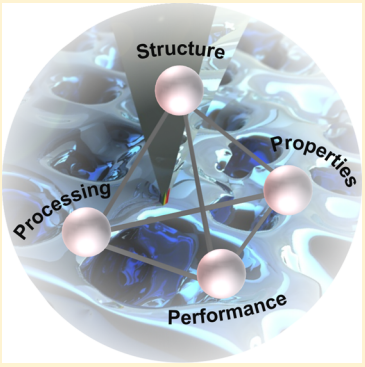

Renewable energy is expected to become a significant percentage of the global energy sources as the total amount of power consumed globally continues to increase each year. Of the renewable resources available, solar is the only one that can deliver the >184 000 TWh per annum required to meet the worldwide energy needs by 2020.[1] Nevertheless, effective high-efficiency *and* low-cost photovoltaics (PV) are still necessary to successfully replace fossil fuel-based technologies. While single-crystalline PV materials generally outperform their polycrystalline counterparts,[2] the extremely high cost associated with their epitaxial fabrication methods is still a barrier to implementation. Nonepitaxial compounds, such as hybrid perovskites and thin-film polycrystalline materials, are very promising alternatives, but improvement in device stability and power conversion efficiency (η) are still required for successful deployment, as will be discussed in detail in this Perspective.

The absorbing layer of halide hybrid perovskites and of most polycrystalline materials for PV (CdTe, CIGS, CZTS, and polycrystalline GaAs) is composed of grains in the microscale range, as shown in Figure 1, with well-defined facets, interfaces, and boundaries. The macroscopic performance of the devices strongly depends on these mesoscale constructs, where the behavior of the average density of atoms corresponding to length scales of 5−50 nm (and to a volume commonly comprised of thousands of atoms) is more relevant than the contribution of the individual atoms themselves.[3] Thus, it is imperative to resolve the performance of the device at similar length scales. While conventional electrical characterization methods are extremely useful, they do not provide information about how each grain and interface contributes to/affects the electrical and optical responses of the PV devices. Scanning probe microscopy (SPM) and scanning (transmission) electron microscopies (STEM and SEM) have been successfully applied to characterize materials for solar cells with high spatial resolution.[4−6] Recently, microscopic techniques have been combined to investigate the structural, optical, chemical, and electrical properties of a variety of relevant materials.[7,8] However, the nanoscale functional imaging of critical mesoscale phenomena in PV materials and in operando devices is still missing. The performance of PV devices is defined by their main figures-of-merit: open-circuit voltage (V_{oc}), short-circuit current density (J_{sc}), fill factor (FF), and η. Thus, the ability to map these quantities with nanoscale spatial resolution will likely unravel the intricate physical and chemical processes that define device functionality at the mesoscale, elucidating the origin of the modest performance of some technologies and of the light-induced chemical reactions that take place in perovskites.

In this Perspective, we first highlight the most promising materials for high-efficiency and low-cost solar cells, including halide hybrid perovskites, CdTe, CIGS, CZTS, and pc-GaAs. Second, we evaluate how cutting-edge functional nanoimaging

Received: May 5, 2017
Accepted: July 7, 2017
Published: July 7, 2017

DOI: 10.1021/acsenergylett.7b00382
ACS Energy Lett. 2017, 2, 1825−1834

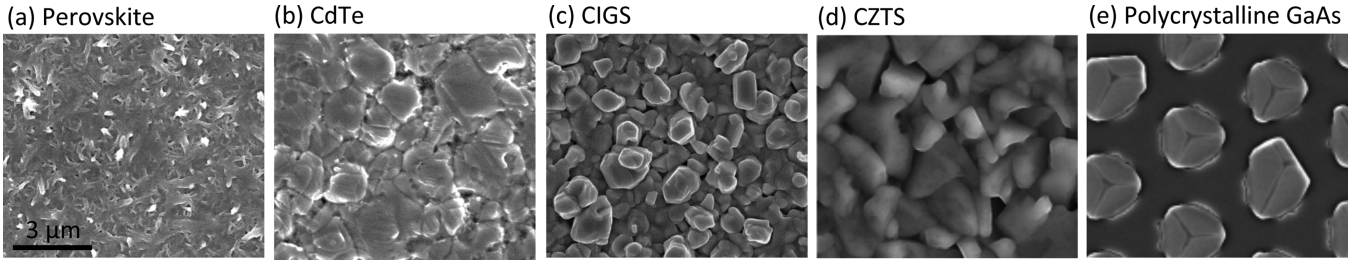

Figure 1. SEM images of selected polycrystalline materials for PV highlighted in this Perspective: (a) hybrid perovskites, reprinted from ref 9, (b) CdTe, (c) CIGS, (d) CZTS, reprinted from ref 10, and (e) polycrystalline GaAs, reprinted from ref 11. In all cases, the absorbing layer is composed of micron-sized grains or smaller, where their optical and electrical responses vary on the same length scale.

The macroscopic performance of nonuniform PV devices strongly depends on their mesoscale constructs, where the behavior of the average density of atoms corresponding to length scales of 5−50 nm is more relevant than the contribution of the individual atoms themselves.

methods can be implemented to advance our understanding of the fundamental physical and chemical processes governing these nonuniform materials, including the use of both electrons and photons as the excitation source for charge carriers. Third, we discuss the need for real-time microscopic methods to probe the degradation mechanisms of perovskite solar cells, still not well understood. Finally, we briefly analyze the relevance of big data to effectively correlate the information acquired by a set of microscopic methods.

Thin Film Materials and Hybrid Perovskites for PV: Opportunities and Current Limitations A complete description of electron and hole generation, recombination, and collection throughout the granular structure of perovskites and polycrystalline thin films can potentially enable us to rationally design the next generation of higher-efficiency PV. Without this critical information, one cannot explain nor control the operating mechanisms that will ultimately help improve device performance and stability. Before discussing the opportunities associated with functional and correlative microscopy to advance the state-of-knowledge of emerging PV technologies, we summarize below the major advantages and challenges of the selected nonuniform solar cell materials.

(i) Hybrid Organic−Inorganic Perovskites. Since 2009, the research community has witnessed the rise of hybrid halide perovskites as a competitive PV technology.[12−14] The perovskite material has the chemical formula ABX_3, where A is an organic cation (most commonly used is methylammonium (MA), CH_3NH_3), B is an inorganic cation (typically Pb or Sn[15]), and X is a halide (typically iodine, but chloride and bromide have also been used). The interchangeability of elements within the compound enables bandgap energy (E_g) tuning from 1.6 to 3.2 eV, very appropriate for multijunction designs. At present, perovskites hold a record power conversion efficiency similar to that of CdTe and CIGS, at $\eta = 22.1 \pm 0.7\%$.[16] However, stabilizing the high performance has proven to be a challenge and is one of the main ongoing focuses of research in the field.[17] Scientists have observed the PV characteristics change in a matter of seconds,[6,18] and the primary processes that cause this instability are still under intense debate.[19] Most perovskites are composed of submicron-scale grains (Figure 1a), where spatial variations in their chemical composition resulting from the spin coating deposition process during device fabrication are possibly responsible for the spatial electrical variations reported in the literature[6,20] as well as ion migration. Therefore, imaging electronic charge separation and collection at the numerous interfaces could elucidate the pathways for carrier transport within the material.[21] Full comprehension and control of the time-dependent physical and chemical processes responsible for the commonly observed degradation of perovskites will likely lead to stable, high-efficiency devices. Additionally, by probing the local electrical response of new lead-free perovskite alternatives,[22] the community will ultimately identify which materials are stable under PV operation conditions and, thus, suitable for device development, which is currently unknown.

(ii) CdTe. CdTe/CdS heterojunction solar cells are a mature technology, available on today's PV market. Thus, improving device performance for a well-established technology can significantly impact the associated industry. At present, the power conversion efficiency record of CdTe solar cells is $\eta = 22.1 \pm 0.5\%$, and the maximum module performance is $\eta = 18.6 \pm 0.6\%$.[16] While the J_{sc} of world record devices has practically achieved its maximum, there is a ∼25% gap between the theoretical and the measured V_{oc} of polycrystalline CdTe solar cells; see Table 1. It has been recently shown that single-crystalline CdTe devices (boundaries free) can achieve V_{oc} as high as 1.096 V,[23] corresponding to ∼20% voltage improve-

Table 1. Theoretical vs Experimental Solar Cell Parameters

material	E_g (eV)	$V_{oc,theory}$ (V)[14,38]	$V_{oc,meas}$ (V)[16]	$\frac{V_{oc,meas}}{V_{oc,theory}}$	$J_{sc,theory}$ (mA/cm^2)[14,38]	$J_{sc,meas}$ (mA/cm^2)[16]	$\frac{J_{sc,meas}}{J_{sc,theory}}$	η (%)[16]
perovskite	1.58	1.325	1.105	0.86	27.2	25.0	0.92	22.1 ± 0.7
CdTe	1.45	1.168	0.887	0.76	30.5	30.25	0.99	22.1 ± 0.5
CIGS	1.15	0.890	0.741	0.83	42.1	37.8	0.90	22.6 ± 0.5
CZTS	1.13	0.884	0.513	0.58	43.3	35.2	0.81	12.6 ± 0.3
polycrystalline GaAs	1.42	1.160	0.994	0.89	31.7	23.2	0.73	18.4 ± 0.5

DOI: 10.1021/acsenergylett.7b00382
ACS Energy Lett. 2017, 2, 1825−1834

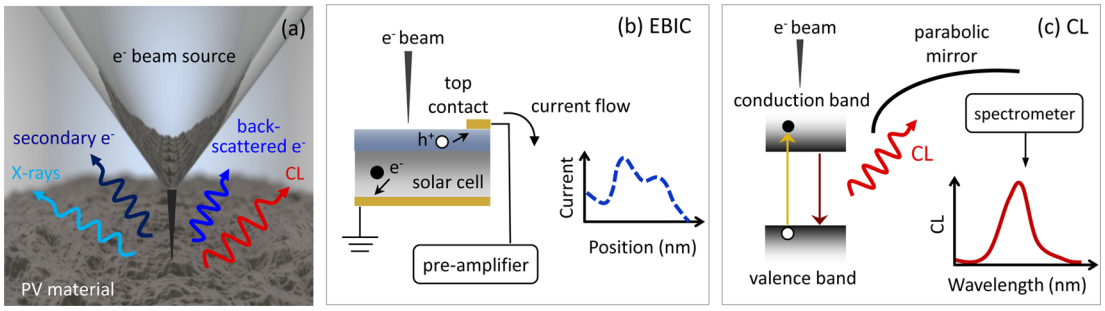

Figure 2. Electrons as a source of excitation for high-resolution functional imaging of solar cells. (a) Illustration of the main radiation signals generated from an e-beam upon interaction with a material. (b) Schematic of EBIC, where the generated current is spatially resolved. (c) Illustration of CL resulting from the radiative recombination of charge carriers.

ment over the best values ever obtained for polycrystalline CdTe solar cells (limited at ~0.9 V, as shown in Table 1). This result strongly indicates that the grain boundaries (GBs) do indeed negatively impact the recombination rate of charge carriers. However, fabricating monocrystalline CdTe thin films is an extremely slow and expensive process. Therefore, identifying and controlling *where* carrier recombination events take place within polycrystalline CdTe will facilitate the design of devices with suppressed nonradiative recombination, higher V_{oc}, and, thus, performance. It has been recently suggested that not every CdTe GB results in voltage reduction;[4,24] thus, the response of individual grains (~1 μm in diameter, as shown in Figure 1b) and their interfaces must be resolved, which requires high spatial resolution electrical measurements.

(iii) $Cu(In_{(1-x)}Ga_x)Se_2$ (CIGS). The extensive characterization of CIGS/CdS heterojunction devices strongly indicates that this material can become a marketable PV technology. Currently, CIGS is the highest-performing thin-film solar cell at $\eta = 22.6 \pm 0.5\%$.[16] The CIGS E_g can be tuned from 1.02 to 1.68 eV as a function of Ga/In content (useful for multijunction approaches), has high optical absorption, is compatible with flexible substrates, and has the potential for low cost/W installation.[25] Nevertheless, the V_{oc} and the J_{sc} of these devices can still be improved, as shown in Table 1. Note that, recently, the J_{sc} of small cells (0.51 cm^2) reached >41 mA/cm^2 (uncertified),[26] approaching the theoretical value. However, its V_{oc} is still >20% below the theoretical prediction. The p-doped CIGS absorbing layer is composed of grains approximately 1 μm in diameter; see Figure 1c. Voltage variations of >20% have been observed despite the uniform chemical composition of the grains.[7] Therefore, enhanced power conversion efficiencies will require mapping how the different grains and interfaces composing the CIGS layer affect charge carrier generation, recombination, and collection. In particular, the possible correlation between the physical behavior of in operando CIGS devices and their structural properties (resulting from a distribution of grain orientations) is still unclear.[25]

(iv) $Cu(Zn,Sn)(S,Se)_2$–CZTS. CZTS belongs to a class of material similar to CIGS (see Figure 1d for grain morphology). The main difference, as the chemical formula suggests, is that the elemental compound does not contain possibly scarce elements like In or Ga and is purposefully restricted to using earth-abundant elements. Here, the Zn and Sn atoms replace the group III elements (In and Ga), producing a structure with a charge-neutral valence state.[27,28] Although extensive efforts to increase the performance of CZTS solar cells, its V_{oc} is 50% below the theoretical prediction for this material (Table 1). Moreover, improvements in the J_{sc} are also still necessary. As a result of its modest V_{oc}, the record device efficiency is $\eta = 12.6 \pm 0.3\%$.[16,29] This lower performance is primarily associated with fabrication of films with high void density or impure phases within the Cu_2ZnSnS_4, such as Sn_xS_y,[30] despite multiple attempts to optimize the thin-film deposition parameters. Determining how these variations in chemical composition affect the local electrical response of CZTS thin films could aid in the fabrication of higher-efficiency devices.

(v) Polycrystalline GaAs. Single-crystalline GaAs offers near-ideal optical and electrical properties. As a result, today's world record single-junction devices are made of monocrystalline GaAs, with power conversion efficiency of $\eta = 28.8 \pm 0.9\%$ under AM1.5 global illumination.[16] Moreover, this semiconductor compound, together with InP and other III–V alloys, has been successfully implemented in high-efficiency multijunction solar cells for concentrator systems and space applications.[31−33] However, the epitaxial fabrication methods required for manufacturing monocrystalline III–V semiconductor modules have prohibitive costs for terrestrial applications. Polycrystalline GaAs is, thus, an attractive alternative to monocrystalline compounds[11] as they can be fabricated as both n- and p-type by close-spaced vapor transport (CSVT); see Figure 1e.[34,35] The record cell efficiency for multicrystalline GaAs is $\eta = 18.4 \pm 0.5\%$,[16] which is significantly below its single-crystalline counterpart and likely due to either the structural defects in the GaAs polycrystals or surface recombination within the distinct facets. By spatially resolving the J_{sc} and V_{oc} of the GaAs mesoscale constructs, we can measure the local response of each crystal facet independently. For instance, it is well-known that the GaAs substrate orientation affects the density of defects.[36,37] Yet, analysis of the contribution of the individual GaAs polycrystals to charge carrier recombination and collection and, therefore, to the overall device performance is critical and still missing.

From Table 1, it is evident that there is an opportunity for material scientists, electrical engineers, physicists, and chemists to advance the state-of-knowledge of perovskites and polycrystalline materials for PV. As the mesoscale constructs strongly influence the efficiency of charge carrier generation, recombination, and collection events, it is imperative that we resolve the performance of these materials/devices at similar length scales. We suggest the implementation of high spatial resolution microscopy methods beyond their standard operation mode as a functional imaging platform to directly resolve the role of the grains and interfaces on solar cell performance. To emulate PV device operation conditions, both electrons and photons can be employed as the carrier excitation

DOI: 10.1021/acsenergylett.7b00382
ACS Energy Lett. 2017, 2, 1825−1834

Table 2. Selected Nanoscale Functional Imaging Methods Performed on PV Materials along with Their Primary Applications and Limitations

imaging technique	applications	limitations
	Electrons as a Source of Excitation	
EBIC	maps of generated current	e-beam induced artifacts due to sample damage, strong dependence on accelerating voltage, primarily a surface signal[46]
CL	radiative recombination of charge carriers	resolution is limited to e-beam volume interaction and excess carrier diffusion
	Photons as a Source of Excitation	
pcAFM	photocurrent, relative nanoscale $I-V$ characterization	removal of conductive coating on probe due to sample contact, slow scan speeds, and effect of contact size
illuminated-KPFM	quantitative, nanoscale V_{oc}	topographic artifacts due to surface roughness
NSOM LBIC	photocurrent beyond diffraction limit	decouple the evanescent field around probe aperture and near-field sample−probe interactions
NSOM PL	radiative recombination of charge carriers beyond diffraction limit	
Tr-PL through NSOM	minority carrier lifetime with subwavelength spatial resolution	

source. Therefore, we discuss the primary advantages and limitations of selected microscopy approaches and how they can be modified to offer quantitative information about device figures-of-merit at the nanoscale.

Electrons as a Source of Excitation. Electron microscopy has proven to be an indispensable tool to acquire structural, electrical, and chemical information on PV materials with nanoscale and atomic spatial resolution. SEM-based measurements are typically performed in a high-vacuum atmosphere, minimizing sample contamination. The interaction of the electron beam (e-beam) with the material can generate secondary and backscattered electrons, X-rays, and cathodoluminescence (CL), portrayed in Figure 2a. A commonly used electrical measurement in SEM is termed the electron-beam-induced current (EBIC), where the e-beam acts as a local source of excitation of carriers, Figure 2b. As the e-beam rasters across the sample, it produces a map of the generated current with spatial resolution primarily determined by the beam size.[39] This characterization method is frequently performed on cross sections to determine the relative changes in charge carrier collection across p−n junctions and other important interfaces. These measurements are especially important for perovskite devices as they do not have a conventional, well-defined p−n junction. However, the use of electrons as the carrier excitation source is prone to severe image artifacts, mainly caused by (i) the e-beam penetration path and depth and (ii) damage to the sample.

CL is the physical phenomenon defined by the emission of photons (electromagnetic radiation) within the UV−IR range, occurring when electrons relax to their fundamental state, resulting from material excitation by an e-beam;[40,41] see the representation in Figure 2c. Thus, information about where radiative recombination takes place within a PV material can be obtained by CL. The spatial resolution is, in principle, defined by the size of the e-beam in the SEM. CL imaging has been implemented in the investigation of a variety of solar cell materials.[42−45] The successful acquisition of reliable data heavily depends on the instrumentation used for light detection. A parabolic mirror, inserted between the specimen and the pole piece, focuses the photons emitted from the solar cell into a well-defined point on the detection system. Then, the collected radiation is spectrally analyzed/resolved for every e-beam position using a high-sensitivity CCD detector, and a two-dimensional emission map is recorded. In this manner, the spectrally and spatially resolved optical response is acquired. CL has recently been implemented to probe the optical response of fully processed devices. As an example, $CdCl_2$ treatment during CdTe solar cell fabrication has been shown to reduce nonradiative recombination in all types of GBs as the overall intensity of the CL spectrum increases after this passivation step.[24] One unique feature of CL is the fact that it does not require device processing. In other words, electrical contacts are not required for mapping the radiative recombination rate of carriers within a thin film. Nevertheless, similar to EBIC, it suffers from the same limitations (see Table 2), mostly caused by the e-beam, used here as the excitation source.

Though the imaging methods described above have been extensively used to characterize nonuniform solar cell materials, a combinatorial SEM-based *functional* imaging platform is necessary to describe the full picture of the fundamental physics of charge carriers. Thus, both EBIC and CL are beginning to be used in conjunction with other SEM-based imaging capabilities to gain information about additional material properties (e.g., chemical or structural). X-rays produced by the e-beam (Figure 2a) are used for compositional mapping, by employing energy dispersive X-ray spectroscopy (EDX).[47] Alternative chemical imaging techniques include electron energy loss spectroscopy (EELS)[39] and time-of-flight secondary-ion mass spectroscopy (ToF-SIMS).[8] Additionally, the orientation of the grains and the types of interfaces present in a sample can be mapped by electron backscattering diffraction (EBSD). Recently, EBIC, transmission electron microscopy with selected area diffraction (TEM-SAD), and atom probe tomography (APT) were united to investigate the $CdSe_xTe_{1-x}$ alloy that forms upon annealing of CdTe devices.[5] Here, the zinc blende phase showed superior photoresponse when compared to wurzite. Although very informative, EBIC measurements do not provide quantitative information regarding current collection nor has the generated current been compared to macroscopic light current−voltage ($I-V$) measurements.

We foresee correlative SEM and TEM approaches becoming widespread over the coming years as the dynamics of the charge carrier processes responsible for high (low) PV performance is strongly related to the structural and chemical characteristics of the grains composing the thin-film devices. To date, most of the work using SEM techniques has focused on capturing the relative variations in current; however, measurements of J_{sc}, a key figure-of-merit for solar cells, are still missing. While a photon generates only one electron−hole pair, an electron can generate up to thousands of electron−hole pairs. The volume

DOI: 10.1021/acsenergylett.7b00382
ACS Energy Lett. 2017, 2, 1825−1834

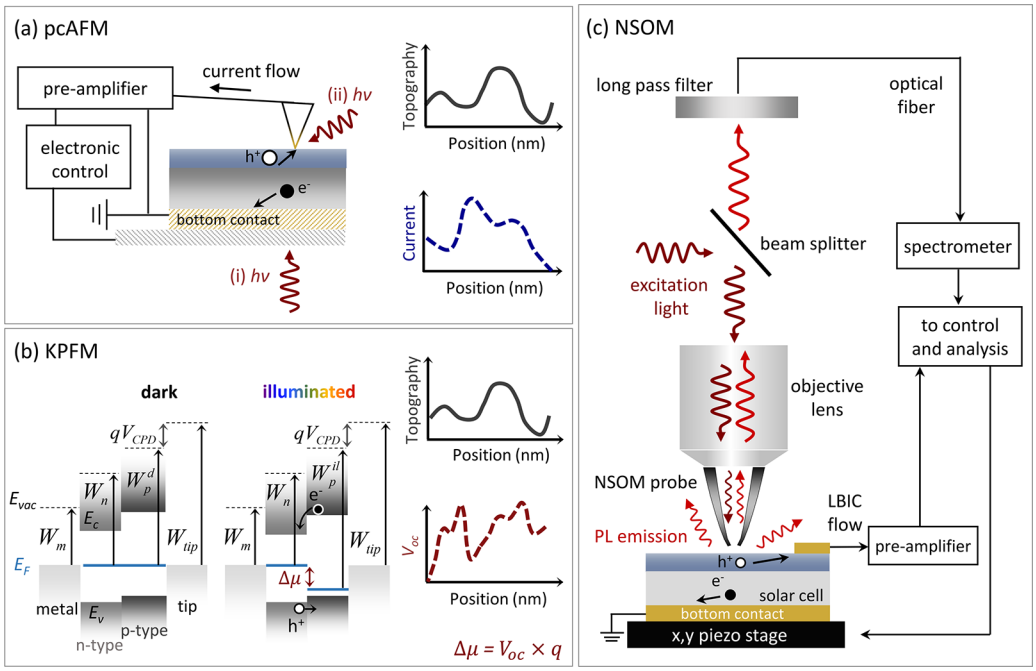

Figure 3. Photons as a source of excitation to nanoimage PV functionality through SPM. (a) In pcAFM, a conductive probe acts as a local electrical contact. An external light source is used, where the illumination direction, (i) or (ii), depends on device configuration. Both the surface topography and current are measured simultaneously. (b) Kelvin probe force microscopy (KPFM) measures the work function (W) difference (or contact potential difference, V_{CPD}) between the probe and the sample surface when grounded with respect to one another. In the dark, *d*, the solar cell is in equilibrium, and all of the Fermi levels are equal. Under illumination (*il*) there is a splitting of the quasi-Fermi level ($\Delta\mu$). The V_{oc} is, thus, determined by subtracting dark- from light-KPFM scans. E_{vac}, E_c, E_{Fn}, E_{Fp}, and E_v denote the vacuum, conduction, the quasi-Fermi level for e^- and h^+ and valence band energies, respectively. Adapted from ref 4. (c) NSOM schematic showing two possible types of measurements with spatial resolution beyond the diffraction limit: photoluminescence (PL) and laser-beam-induced current (LBIC) microscopy.

in which the carrier excitation event occurs depends on the e-beam current and voltage, the material density, the bandgap energy, its backscatter coefficient, the atomic weight, the atomic number, and the quantum efficiency for generating an electron–hole pair.[48] Thus, the volume of excitation, which is defined by the trajectory of the electrons within the solid, must be calculated for a quantitative comparison between EBIC and J_{sc}. For that, the role of the contact size must also be taken into consideration.[49] Although the contribution of each individual atom is not as relevant as the mesoscale behavior of the material, if atomic resolution becomes needed, we expect TEM-based EBIC to be implemented. In this case, besides all considerations mentioned above, one must also determine the possible overestimated contribution of surface recombination due to the very large surface area-to-volume ratio of the samples (as a result of the lamella sample size).

Photons as a Source of Excitation. The nanoscale functional imaging of PV using photons as the excitation source requires researchers to use atomic force microscopy (AFM) or near-field scanning optical microscopy (NSOM). Both platforms offer spatial resolution beyond the diffraction limit, <100 nm, enabling elucidation of the local electrical and optical properties of solar cells. In this section of the Perspective, we summarize the operation principles of selected AFM- and NSOM-based methods that provide invaluable insights about the material optoelectronic response and focus on how they can provide *quantitative* information about the figures-of-merit of the solar cells, with nanoscale spatial resolution.

SPM methods have demonstrated exceptional versatility when mapping the electrical response of PV with nanometer spatial resolution.[4,50] Briefly, in AFM, a deflection laser shines light onto the probe, which is reflected back onto a photodiode detector. The coordinates of this laser are sent to a feedback loop in the microscope controller, which adjusts the height of the cantilever (and probe) and the *x,y* scan stage position. Force–distance curves and the surface topography of the sample are acquired by evaluating the probe–sample interactions. A common AFM mode used to determine the electrical response of solar cells is photoconductive (pc)AFM. Here, a conductive metal probe acts as the top local electrical contact of the PV device, as illustrated in Figure 3a. Upon device illumination by an external light source, the probe directly collects the generated photocurrent while recording the topography of the sample in contact mode. The potential beneficial role of GBs in CdTe, CIGS, and CZTS devices as current collectors has been broadly investigated through pcAFM.[51−53] However, it is still unknown how the GBs affect charge carrier recombination, which requires mapping V_{oc}, as will be discussed later. pcAFM has been applied to perovskites[54] and recently integrated with voltage biasing to produce spatially resolved "*I*–*V* curves" of the devices.[20] In these measurements, individual maps of *I*–*V* parameters can be obtained, extremely valuable to estimate relative changes in all figures-of-merit, with nanoscale spatial resolution. In order to translate this information into macroscopic device parameters, one needs to take into consideration (1) the extremely small volume of excitation when light focusing is used, (2) the effect of the probe size as a current collector and charge carrier diffusion length, (3) the photon flux in single-wavelength measurements, (4) spatial variations in the absorption

DOI: 10.1021/acsenergylett.7b00382
ACS Energy Lett. 2017, 2, 1825−1834

coefficient of the material under investigation (which will necessarily affect charge carrier generation), and (5) the possible optical losses of the experimental setup.

While extensive efforts have been made to increase the J_{sc} of thin-film polycrystalline solar cells, higher efficiencies are still limited by the V_{oc} (see Table 1). The local variations of V_{oc} within these materials can be determined by a much less explored and equally powerful AFM-based method: Kelvin probe force microscopy (KPFM).[4,6] Here, the work function difference between the sample surface and the probe is measured, as illustrated in Figure 3b. By subtracting an illuminated KPFM scan from a dark one, the quasi-Fermi level splitting ($\Delta\mu$) and, therefore, the local V_{oc} generated by the material are obtained. This universal approach only requires a half-processed device and can be performed in ambient conditions. With proper system calibration, the quantitative V_{oc} obtained from focused illumination is converted into a 1 sun V_{oc} map under AM1.5 global illumination. We anticipate V_{oc} mapping through KPFM to be combined with pcAFM (on the very same grains and boundaries) to quantify *where* charge carrier recombination and collection take place, respectively. Combined, these measurements enable the deconvolution of both processes, critical to identify which mechanism is limiting the performance of the device under investigation. Further, by implementing a correlative microscopy approach, where the SPM methods are combined with ex situ EBSD, one can elucidate which interfaces and grain orientations in polycrystalline materials are responsible for the modest V_{oc} of the technologies discussed earlier.

Functional imaging through NSOM has been applied less frequently to solar cells when compared to AFM-based methods. Here, evanescent waves are used to break the far-field diffraction limit. By keeping the distance between the probe and the sample surface considerably smaller than the wavelength of light (at least 2 orders of magnitude), it is possible to map the solar cells' optical response with true nanoscale spatial resolution. In NSOM, a probe or an optical fiber with a hollow center (60−200 nm in diameter) is used as the excitation and/or collection source, as depicted in Figure 3c. One electrical measurement option using NSOM is laser-beam-induced current (LBIC). In this configuration, the photons transmitted through the probe induce photocurrent in a highly localized region of the solar cell. This method has been applied to identify the diffusion of sulfur in CdTe[55] and to spatially resolve the external quantum efficiency (EQE) of CdTe solar cells, determining the contribution of grains and boundaries to the overall signal of the device[56−58] and the photoresponse of grain and GBs in CIGS.[59] For quantitative comparison between the LBIC signal and the macroscopic J_{sc} of a device, one must accurately determine the contribution of the dark saturation current of the entire sample (whole device area) and extricate possible topographic artifacts due to near-field light coupling. One attractive application of NSOM for perovskites is to realize spectrally dependent LBIC scans to spatially monitor the existence of trap states within the material, where ion migration seems to be a major contributor in their local electrical response.[6]

A powerful alternative measurement is to use the NSOM probe for both the excitation of carriers and the collection of emitted photons (photoluminescence, PL) resulting from radiative recombination. Collection of the PL signal strongly depends on light−probe coupling, and considerable effort has focused on designing optimized probes for capturing the emitted photons. For instance, campanile tips have been identified as an excellent geometry to enhance the coupling efficiency between far and near fields, allowing for PL signal imaging of nanoscale features in InP nanowires for PV applications.[60] PL microscopy with nanoscale spatial resolution can be realized to probe the impact of GaAs polycrystals' facets on carrier recombination. Note that device processing is not required here. Different than InP, GaAs is a material that is not self-passivated. Thus, one could use PL through NSOM to identify the effect of distinct surface passivation processes (e.g., Na_2S and Si_3N_4) on the recombination rate within the different facets composing the GaAs polycrystals. Although unconventional, NSOM can also be integrated into SEM. In this dual-probe approach, the NSOM tip collects the near-field CL emission caused by the e-beam to image the energy transport mechanisms without being limited by photon recycling or excess carrier diffusion.[61] We foresee that combining LBIC and PL signals with simulations of the electrodynamics at the near-field regime could enable a tomography of charge carrier generation, recombination, and collection, resolving the role of the mesoscale constructs within polycrystalline solar cells on their macroscopic device performance.

Time-resolved PL (tr-PL) is an extremely powerful method to quantify the minority carriers' lifetime within a material. Here, the carriers that recombine radiatively (PL signal) are detected by a time-correlating photon counting system. tr-PL spectroscopy has been widely implemented to resolve the effect of passivation methods on the lifetime of polycrystalline materials for PV,[62,63] as well as the role of precursor solution concentration (and band gap) in halide perovskites.[64,65] When combined with a NSOM microscope, it provides maps of the temporal dynamics of the PL signal, with subwavelength spatial resolution. tr-PL through confocal optical microscopy[66,67] or NSOM[68] could be implemented to investigate the spatial distribution of minority carrier lifetimes in perovskite grains and its photoinstability. A primary advantage of tr-PL microscopy is that it enables measurements in a film, not requiring any device processing.

> The nanospectroscopy of polycrystalline solar cells through NSOM, combined with full-field simulations, could enable a tomography of charge carrier generation, recombination, and collection, resolving the role of the mesoscale constructs to their macroscopic device performance.

Probing the Degradation of Perovskite Solar Cells. The commonly observed degradation of perovskite solar cells is the main barrier for this emerging material to become a reliable PV technology. Thus, measuring and controlling the physical and chemical processes responsible for the transient electrical behavior of perovskites is critical for its widespread deployment.[6,19] We foresee pcAFM and illuminated KPFM being implemented to track material degradation. For instance, $MAPbX_3$ (X = Br or I) is unstable under illumination, can suffer from structural phase transition at low temperatures (<60 °C), and often degrades upon exposure to moisture.[69] Thus, SPM under controlled illumination, humidity, and temperature

DOI: 10.1021/acsenergylett.7b00382
ACS Energy Lett. 2017, 2, 1825−1834

conditions will help elucidate the driving forces behind the material degradation commonly observed in perovskites. For example, spectrally dependent KPFM will likely reveal the possible presence of trap states within the material and how their density varies from grain to grain. The reversibility of the electrical response of perovskites can also be probed by tuning the humidity (low, high, low) upon sequential SPM measurements. Here, pcAFM and KPFM could resolve how both J_{sc} and V_{oc} change as the perovskite is exposed to moisture. The advantage of using microscopic methods to probe perovskite solar cells lies in quantifying spatial variations within the samples, which could be associated with chemical composition deviations from grain to grain.

The *dynamic* electrical behavior of the perovskites has been measured both in plane-view and in cross section by pcAFM[70] and KPFM.[6,71] However, there is still a pressing need for scientists to discover the driving forces responsible for the devices' transient behavior when the material is exposed to light and humidity. In our opinion, this dynamic response requires further development of time-dependent functional microscopy methods that will provide four-dimensional (4D) information, space and time, at relevant length scales. Mimicking realistic operation conditions (including the environment) of perovskite devices during operando measurements is necessary to identify *why* and *how* the material is degrading. Preferably, these 4D measurements should be combined with chemical imaging to establish a correlation between device behavior and the changes in chemical composition. The combination of illuminated KPFM (as described earlier) with Raman imaging and other AFM-based chemical mapping is a promising route to elucidate the effect of photoinduced chemical reactions in device degradation. As recently demonstrated,[6] fast KPFM scans (16 s/frame) that allow *real-time* measurements of local V_{oc} have revealed (1) substantial ion migration during perovskites' illumination and (2) a residual postillumination voltage resulting from a time-dependent ion migration current, never measured before. These fast scans can be extended to lead-free perovskite films,[72] for example, $MASnI_3$[73] or $Cs_2BiAgCl_6$,[22] as well as new compounds for multijunction PV, such as $Rb-FA_{0.75}MA_{0.15}Cs_{0.1}PbI_2Br$,[74] to determine their dynamic response and, thus, material stability when exposed to light.

> The hallmark transient electrical behavior of perovskites requires the further development of four-dimensional, space and time, functional microscopy methods to quantify device degradation at relevant length scales.

Correlative Microscopy and the Need for Big Data Analytics. We foresee that the use of combined functional imaging microscopies will produce large amounts of data that must be effectively analyzed for an understanding of the material behaviors. An emerging investigation pathway is "big data", which encompasses the analysis of all data to identify critical patterns and associations (e.g., correlation between GBs and low V_{oc}). Big data analytics involves evaluating the detected signals with approaches from multivariate statistics and machine learning to identify meaningful relationships between material properties, obtained from a set of microscopy measurements in this case.[75] Ultimately, the main advantage of the available paradigms[76] is to gain insight into complex phenomena while minimizing computational time. For example, using principal component analysis (PCA),[77] one can determine which dimensions of the data account for the most variance in an imaging data set. Note that in this situation each physical quantity is assigned as one data dimension. This method has already proven useful when combined with band excitation magnetic force microscopy; PCA provided the same qualitative insight as the simple harmonic oscillator model while requiring $\sim 10^4$ less computation time.[77] Machine learning approaches will likely help scientists determine which defects and GBs in polycrystalline PV materials contribute most to performance deficiencies. For instance, a combination of NSOM LBIC and ex situ EBSD data acquired at the same region of a sample could train an algorithm to predict the electrical signal based solely on the angle between two adjacent GBs. Data mining may also identify degradation mechanisms in perovskite solar cells. Namely, factor analysis can be applied to a combination of illuminated KPFM and tip-enhanced Raman spectroscopy under a controlled atmosphere to establish how the electrical and chemical responses vary as a function of relative humidity. Further, time-dependent photocurrent and photovoltage measurements of emerging lead-free perovskite alternatives could provide a roadmap for stable materials. For the reasons outlined, we anticipate the use of big data analytics on information produced by combinatorial functional microscopy.

> Machine learning approaches based on big data analytics will likely help scientists determine which defects and grain boundaries in polycrystalline PV materials contribute most to performance deficiencies.

Functional Imaging of Mesoscale Behavior/Phenomena in PV: Looking Forward. In perovskites, device stability is currently the main barrier toward implementing a reliable technology, followed by the pressing need to identify nontoxic lead-free, stable options. The full potential of thin-film polycrystalline materials for PV is primarily limited by their V_{oc}, which is strongly related to nonradiative recombination events within the material. As the grains and boundaries forming the devices are acknowledged to affect their electrical response, it is imperative that we identify which types of grains and interfaces contribute to charge carrier nonradiative recombination. In order to determine the local electrical properties of the mesoscale constituents of both perovskites and inorganic thin-film PV, researchers must implement microscopy techniques beyond their standard operation modes, quantifying the figures-of-merit (and, hence, the device performance) at relevant length scales. Further, the large amount of generated data must be analyzed in an effective manner using approaches based on big data analytics, leading to quantitative information about the devices under investigation.

We expect the realization of correlative microscopy and the functional imaging of materials/devices at the mesoscale to finally elucidate some critical open questions in the field, such as the following: What are the light-induced chemical reactions responsible for perovskites' degradation under 1 sun illumination? What is the role of humidity in perovskite's performance? Which types of interfaces in CdTe, CIGS, and CZTS are

DOI: 10.1021/acsenergylett.7b00382
ACS Energy Lett. 2017, 2, 1825−1834

responsible for the low carrier radiative recombination rate that limits their V_{oc}? How do the different facets composing GaAs polycrystals affect charge carrier generation, recombination, and collection? Is the diode ideality factor for all GBs the same in a polycrystalline PV device? To answer these questions, among many others, it is essential to determine the physical behavior of the mesoscale constructs when the devices are in operando. Functional imaging methods will likely act as the central "covalent bond" between the materials science structure−properties−processing−performance tetrahedron cornerstones, providing unprecedented correlative insights into materials for PV at the mesoscale. In turn, these sophisticated measurements can potentially allow rational design of higher-performance PV devices based on low-cost materials/methods.

AUTHOR INFORMATION

Corresponding Author

*E-mail: mleite@umd.edu.

ORCID

Elizabeth M. Tennyson: 0000-0003-0071-8445
John M. Howard: 0000-0002-3990-5478
Marina S. Leite: 0000-0003-4888-8195

Notes

The authors declare no competing financial interest.

Biographies

E. M. Tennyson is currently a Ph.D. student in the Department of Materials Science and Engineering at the University of Maryland and in the Institute for Research in Electronics and Applied Physics (IREAP), College Park. She received her B.S. in Physics from the University of Wisconsin, La Crosse in 2012. Her research focuses on the nanoscale characterization of perovskites and CIGS for photovoltaics.

J. M. Howard is a Ph.D. student in the Department of Materials Science and Engineering and in the Institute for Research in Electronics and Applied Physics (IREAP) at the University of Maryland, College Park. He received his B.S. in both Physics and Mathematics from the University of Massachusetts, Amherst in 2013. His research relies on investigating the optical and electrical properties of polycrystalline materials for solar cells by microscopy methods.

M. S. Leite is an assistant professor in the Department of Materials Science and Engineering and in the Institute for Research in Electronics and Applied Physics (IREAP) at the University of Maryland, College Park. Her group is engaged in fundamental and applied research in materials for energy harvesting and storage, including the realization of novel microscopy methods for the functional imaging of materials at the mesoscale.

ACKNOWLEDGMENTS

The authors thank Dr. M. R. S. Dias, C. Gong, and W. B. Gunnarsson for fruitful discussions. Financial support from NSF-ECCS (award #16-10833), the 2016 American Physical Society Ovshinsky Sustainability Fellowship, the James A. Clark School of Engineering, the 2015 RASA Award, the 2015 UMD Graduate School Summer Research Fellowship, and the 2016 UMD Graduate Dean's Dissertation Fellowship are graciously acknowledged.

REFERENCES

(1) *International Energy Outlook 2016*; U.S. Energy Information Administration, 2016.

(2) Green, M. A.; Bremner, S. P. Energy Conversion Approaches and Materials for High-Efficiency Photovoltaics. *Nat. Mater.* **2016**, *16*, 23−34.

(3) *From Quanta to the Continuum: Opportunities for Mesoscale Science*, Report of US Department of Energy Basic Energy Sciences Advisory Committee; 2012.

(4) Tennyson, E. M.; Garrett, J. L.; Frantz, J. A.; Myers, J. D.; Bekele, R. Y.; Sanghera, J. S.; Munday, J. N.; Leite, M. S. Nanoimaging of Open-Circuit Voltage in Photovoltaic Devices. *Adv. Energy Mater.* **2015**, *5*, 1501142.

(5) Poplawsky, J. D.; Guo, W.; Paudel, N.; Ng, A.; More, K.; Leonard, D.; Yan, Y. Structural and Compositional Dependence of the $CdTe_xSe_{1-x}$ Alloy Layer Photoactivity in CdTe-Based Solar Cells. *Nat. Commun.* **2016**, *7*, 12537.

(6) Garrett, J. L.; Tennyson, E. M.; Hu, M.; Huang, J.; Munday, J. N.; Leite, M. S. Real-Time Nanoscale Open-Circuit Voltage Dynamics of Perovskite Solar Cells. *Nano Lett.* **2017**, *17*, 2554−2560.

(7) Tennyson, E. M.; Frantz, J. A.; Howard, J. M.; Gunnarsson, W. B.; Myers, J. D.; Bekele, R. Y.; Sanghera, J. S.; Na, S.-M.; Leite, M. S. Photovoltage Tomography in Polycrystalline Solar Cells. *ACS Energy Lett.* **2016**, *1*, 899−905.

(8) deQuilettes, D. W.; Zhang, W.; Burlakov, V. M.; Graham, D. J.; Leijtens, T.; Osherov, A.; Bulovic, V.; Snaith, H. J.; Ginger, D. S.; Stranks, S. D. Photo-Induced Halide Redistribution in Organic-Inorganic Perovskite Films. *Nat. Commun.* **2016**, *7*, 11683.

(9) Xie, Y.; Shao, F.; Wang, Y.; Xu, T.; Wang, D.; Huang, F. Enhanced Performance of Perovskite $CH_3NH_3PbI_3$ Solar Cell by Using CH_3NH_3I as Additive in Sequential Deposition. *ACS Appl. Mater. Interfaces* **2015**, *7*, 12937−12942.

(10) Son, D.-H.; Kim, D.-H.; Park, S.-N.; Yang, K.-J.; Nam, D.; Cheong, H.; Kang, J.-K. Growth and Device Characteristics of CZTSSe Thin-Film Solar Cells with 8.03% Efficiency. *Chem. Mater.* **2015**, *27*, 5180−5188.

(11) Greenaway, A. L.; Sharps, M. C.; Boucher, J. W.; Strange, L. E.; Kast, M. G.; Aloni, S.; Boettcher, S. W. Selective Area Epitaxy of GaAs Microstructures by Close-Spaced Vapor Transport for Solar Energy Conversion Applications. *ACS Energy Lett.* **2016**, *1*, 402−408.

(12) Kojima, A.; Teshima, K.; Shirai, Y.; Miyasaka, T. Organometal Halide Perovskites as Visible-Light Sensitizers for Photovoltaic Cells. *J. Am. Chem. Soc.* **2009**, *131*, 6050−6051.

(13) Seo, J.; Noh, J. H.; Seok, S. I. Rational Strategies for Efficient Perovskite Solar Cells. *Acc. Chem. Res.* **2016**, *49*, 562−572.

(14) Nayak, P. K.; Bisquert, J.; Cahen, D. Assessing Possibilities and Limits for Solar Cells. *Adv. Mater.* **2011**, *23*, 2870−2876.

(15) Song, T.-B.; Yokoyama, T.; Aramaki, S.; Kanatzidis, M. G. Performance Enhancement of Lead-Free Tin-Based Perovskite Solar Cells with Reducing Atmosphere-Assisted Dispersible Additive. *ACS Energy Lett.* **2017**, *2*, 897−903.

(16) Green, M. A.; Emery, K.; Hishikawa, Y.; Warta, W.; Dunlop, E. D.; Levi, D. H.; Ho-Baillie, A. W. Y. Solar Cell Efficiency Tables (version 49). *Prog. Photovoltaics* **2017**, *25*, 3−13.

(17) Bisquert, J.; Qi, Y.; Ma, T.; Yan, Y. Advances and Obstacles on Perovskite Solar Cell Research from Material Properties to Photovoltaic Function. *ACS Energy Lett.* **2017**, *2*, 520−523.

(18) Tress, W.; Marinova, N.; Moehl, T.; Zakeeruddin, S. M.; Nazeeruddin, M. K.; Gratzel, M. Understanding the Rate-Dependent J-V Hysteresis, Slow Time Component, and Aging in $CH_3NH_3PbI_3$ Perovskite Solar Cells: The Role of a Compensated Electric Field. *Energy Environ. Sci.* **2015**, *8*, 995−1004.

(19) Berry, J.; Buonassisi, T.; Egger, D. A.; Hodes, G.; Kronik, L.; Loo, Y.-L.; Lubomirsky, I.; Marder, S. R.; Mastai, Y.; Miller, J. S.; et al. Hybrid Organic-Inorganic Perovskites (HOIPs): Opportunities and Challenges. *Adv. Mater.* **2015**, *27*, 5102−5112.

(20) Kutes, Y.; Zhou, Y.; Bosse, J. L.; Steffes, J.; Padture, N. P.; Huey, B. D. Mapping the Photoresponse of $CH_3NH_3PbI_3$ Hybrid Perovskite Thin Films at the Nanoscale. *Nano Lett.* **2016**, *16*, 3434−3441.

(21) Edri, E.; Kirmayer, S.; Mukhopadhyay, S.; Gartsman, K.; Hodes, G.; Cahen, D. Elucidating the Charge Carrier Separation and Working

DOI: 10.1021/acsenergylett.7b00382
ACS Energy Lett. 2017, 2, 1825−1834

Mechanism of $CH_3NH_3PbI_{3-x}Cl_x$ Perovskite Solar Cells. *Nat. Commun.* **2014**, *5*, 4461.
(22) Giustino, F.; Snaith, H. J. Toward Lead-Free Perovskite Solar Cells. *ACS Energy Lett.* **2016**, *1*, 1233−1240.
(23) Zhao, Y.; Boccard, M.; Liu, S.; Becker, J.; Zhao, X.-H.; Campbell, C. M.; Suarez, E.; Lassise, M. B.; Holman, Z.; Zhang, Y.-H. Monocrystalline CdTe Solar Cells with Open-Circuit Voltage Over 1 V and Efficiency of 17%. *Nat. Energy* **2016**, *1*, 16067.
(24) Moseley, J.; Metzger, W. K.; Moutinho, H. R.; Paudel, N.; Guthrey, H. L.; Yan, Y.; Ahrenkiel, R. K.; Al-Jassim, M. M. Recombination by Grain-Boundary Type in CdTe. *J. Appl. Phys.* **2015**, *118*, 025702.
(25) Abou-Ras, D.; Schmidt, S. S.; Schäfer, N.; Kavalakkatt, J.; Rissom, T.; Unold, T.; Mainz, R.; Weber, A.; Kirchartz, T.; Simsek Sanli, E.; et al. Compositional and Electrical Properties of Line and Planar Defects in $Cu(In,Ga)Se_2$ Thin Films for Solar Cells. *Phys. Status Solidi RRL* **2016**, *10*, 363−375.
(26) Kamada, R.; Yagioka, T.; Adachi, S.; Handa, A.; Tai, K. F.; Kato, T.; Sugimoto, H. New World Record $Cu(In, Ga)(Se, S)_2$ Thin Film Solar Cell Efficiency Beyond 22%. *2016 IEEE 43rd Photovoltaic Specialists Conference (PVSC)* **2016**, 1287−1291.
(27) Walsh, A.; Chen, S.; Wei, S.-H.; Gong, X.-G. Kesterite Thin-Film Solar Cells: Advances in Materials Modelling of Cu_2ZnSnS_4. *Adv. Energy Mater.* **2012**, *2*, 400−409.
(28) Polizzotti, A.; Repins, I. L.; Noufi, R.; Wei, S.-H.; Mitzi, D. B. The State and Future Prospects of Kesterite Photovoltaics. *Energy Environ. Sci.* **2013**, *6*, 3171−3182.
(29) Wang, W.; Winkler, M. T.; Gunawan, O.; Gokmen, T.; Todorov, T. K.; Zhu, Y.; Mitzi, D. B. Device Characteristics of CZTSSe Thin-Film Solar Cells with 12.6% Efficiency. *Adv. Energy Mater.* **2014**, *4*, 1301465.
(30) Su, C.-Y.; Yen Chiu, C.; Ting, J.-M. Cu_2ZnSnS_4 Absorption Layers with Controlled Phase Purity. *Sci. Rep.* **2015**, *5*, 9291.
(31) Leite, M. S.; Woo, R. L.; Hong, W. D.; Law, D. C.; Atwater, H. A. Wide-Band-Gap InAlAs Solar Cell for an Alternative Multijunction Approach. *Appl. Phys. Lett.* **2011**, *98*, 093502.
(32) Cotal, H.; Fetzer, C.; Boisvert, J.; Kinsey, G.; King, R.; Hebert, P.; Yoon, H.; Karam, N. III-V Multijunction Solar Cells for Concentrating Photovoltaics. *Energy Environ. Sci.* **2009**, *2*, 174−192.
(33) Leite, M. S.; Woo, R. L.; Munday, J. N.; Hong, W. D.; Mesropian, S.; Law, D. C.; Atwater, H. A. Towards an Optimized All Lattice-Matched InAlAs/InGaAsP/InGaAs Multijunction Solar Cell with Efficiency > 50%. *Appl. Phys. Lett.* **2013**, *102*, 033901.
(34) Ritenour, A. J.; Cramer, R. C.; Levinrad, S.; Boettcher, S. W. Efficient n-GaAs Photoelectrodes Grown by Close-Spaced Vapor Transport from a Solid Source. *ACS Appl. Mater. Interfaces* **2012**, *4*, 69−73.
(35) Ritenour, A. J.; Boucher, J. W.; DeLancey, R.; Greenaway, A. L.; Aloni, S.; Boettcher, S. W. Doping and Electronic Properties of GaAs Grown by Close-Spaced Vapor Transport from Powder Sources for Scalable III-V Photovoltaics. *Energy Environ. Sci.* **2015**, *8*, 278−285.
(36) Kamon, K.; Shimazu, M.; Kimura, K.; Mihara, M.; Ishii, M. Orientation Dependence of GaAs Growth in Low-Pressure OMVPE. *J. Cryst. Growth* **1987**, *84*, 126−132.
(37) Hersee, S. D.; Barbier, E.; Blondeau, R.; Blondeau, R. A Study of the Orientation Dependence of Ga(Al)As Growth by MOVPE. *J. Cryst. Growth* **1986**, *77*, 310−320.
(38) Belghachi, A. Theoretical Calculation of the Efficiency Limit for Solar Cells. In *Solar Cells - New Approaches and Reviews*; Kosyachenko, L. A., Ed.; InTech, 2015.
(39) Li, C.; Wu, Y.; Poplawsky, J.; Pennycook, T. J.; Paudel, N.; Yin, W.; Haigh, S. J.; Oxley, M. P.; Lupini, A. R.; Al-Jassim, M.; et al. Grain-Boundary-Enhanced Carrier Collection in CdTe Solar Cells. *Phys. Rev. Lett.* **2014**, *112*, 156103.
(40) Coenen, T.; den Hoedt, S. V.; Polman, A. A New Cathodoluminescence System for Nanoscale Optics, Materials Science, and Geology. *Microsc. Today* **2016**, *24*, 12−19.
(41) Daniel Abou-Ras, T. K.; Rau, U. *Advanced Characterization Techniques for Thin Film Solar Cells*; Wiley-VCH Verlag GmbH & Co, 2011.
(42) Müller, M.; Ribbe, S.; Hempel, T.; Bertram, F.; Christen, J.; Witte, W.; Paetel, S.; Powalla, M. Investigation of Vertical Compositional Gradients in $Cu(In,Ga)Se_2$ by Highly Spatially and Spectrally Resolved Cathodoluminescence Microscopy. *Thin Solid Films* **2013**, *535*, 270−274.
(43) Consonni, V.; Baier, N.; Robach, O.; Cayron, C.; Donatini, F.; Feuillet, G. Local Band Bending and Grain-to-Grain Interaction Induced Strain Nonuniformity in Polycrystalline CdTe Films. *Phys. Rev. B: Condens. Matter Mater. Phys.* **2014**, *89*, 035310.
(44) Bischak, C. G.; Sanehira, E. M.; Precht, J. T.; Luther, J. M.; Ginsberg, N. S. Heterogeneous Charge Carrier Dynamics in Organic−Inorganic Hybrid Materials: Nanoscale Lateral and Depth-Dependent Variation of Recombination Rates in Methylammonium Lead Halide Perovskite Thin Films. *Nano Lett.* **2015**, *15*, 4799−4807.
(45) Dar, M. I.; Jacopin, G.; Hezam, M.; Arora, N.; Zakeeruddin, S. M.; Deveaud, B.; Nazeeruddin, M. K.; Grätzel, M. Asymmetric Cathodoluminescence Emission in $CH_3NH_3PbI_{3-x}Br_x$ Perovskite Single Crystals. *ACS Photonics* **2016**, *3*, 947−952.
(46) Klein-Kedem, N.; Cahen, D.; Hodes, G. Effects of Light and Electron Beam Irradiation on Halide Perovskites and Their Solar Cells. *Acc. Chem. Res.* **2016**, *49*, 347−354.
(47) Guthrey, H.; Johnston, S.; Weiss, D. N.; Grover, S.; Jones, K.; Blosse, A.; Al-Jassim, M. Three-Dimensional Minority-Carrier Collection Channels at Shunt Locations in Silicon Solar Cells. *Sol. Energy* **2016**, *135*, 163−168.
(48) Sempau, J.; Acosta, E.; Baro, J.; Fernández-Varea, J. M.; Salvat, F. An Algorithm for Monte Carlo Simulation of Coupled Electron-Photon Transport. *Nucl. Instrum. Methods Phys. Res., Sect. B* **1997**, *132*, 377−390.
(49) Yoon, H. P.; Haney, P. M.; Ruzmetov, D.; Xu, H.; Leite, M. S.; Hamadani, B. H.; Talin, A. A.; Zhitenev, N. B. Local Electrical Characterization of Cadmium Telluride Solar Cells Using Low-Energy Electron Beam. *Sol. Energy Mater. Sol. Cells* **2013**, *117*, 499−504.
(50) Tuteja, M.; Mei, A. B.; Palekis, V.; Hall, A.; MacLaren, S.; Ferekides, C. S.; Rockett, A. A. $CdCl_2$ Treatment-Induced Enhanced Conductivity in CdTe Solar Cells Observed Using Conductive Atomic Force Microscopy. *J. Phys. Chem. Lett.* **2016**, *7*, 4962−4967.
(51) Lombez, L.; Soro, M.; Delamarre, A.; Naghavi, N.; Barreau, N.; Lincot, D.; Guillemoles, J.-F. Revisiting the Interpretation of Biased Luminescence: Effects on $Cu(In,Ga)Se_2$ Photovoltaic Heterostructures. *J. Appl. Phys.* **2014**, *116*, 064504.
(52) Kutes, Y.; Aguirre, B. A.; Bosse, J. L.; Cruz-Campa, J. L.; Zubia, D.; Huey, B. D. Mapping Photovoltaic Performance with Nanoscale Resolution. *Prog. Photovoltaics* **2016**, *24*, 315−325.
(53) Muhunthan, N.; Singh, O. P.; Toutam, V.; Singh, V. N. Electrical Characterization of Grain Boundaries of CZTS Thin Films using Conductive Atomic Force Microscopy Techniques. *Mater. Res. Bull.* **2015**, *70*, 373−378.
(54) Eperon, G. E.; Moerman, D.; Ginger, D. S. Anticorrelation Between Local Photoluminescence and Photocurrent Suggests Variability in Contact to Active Layer in Perovskite Solar Cells. *ACS Nano* **2016**, *10*, 10258−10266.
(55) Herndon, M. K.; Gupta, A.; Kaydanov, V.; Collins, R. T. Evidence for Grain-Boundary-Assisted Diffusion of Sulfur in Polycrystalline CdS/CdTe Heterojunctions. *Appl. Phys. Lett.* **1999**, *75*, 3503−3505.
(56) Leite, M. S.; Abashin, M.; Lezec, H. J.; Gianfrancesco, A. G.; Talin, A. A.; Zhitenev, N. B. Nanoscale Imaging of Photocurrent and Efficiency in CdTe Solar Cells. *ACS Nano* **2014**, *8*, 11883−11890.
(57) Leite, M. S.; Abashin, M.; Lezec, H. J.; Gianfrancesco, A. G.; Talin, A. A.; Zhitenev, N. B. Mapping the Local Photoelectronic Properties of Polycrystalline Solar Cells Through High Resolution Laser-Beam-Induced Current Microscopy. *IEEE Journal of Photovoltaics* **2014**, *4*, 311−316.
(58) Smith, S.; Zhang, P.; Gessert, T.; Mascarenhas, A. Near-Field Optical Beam-Induced Currents in CdTe/CdS Solar Cells: Direct

DOI: 10.1021/acsenergylett.7b00382
ACS Energy Lett. 2017, 2, 1825−1834

Measurement of Enhanced Photoresponse at Grain Boundaries. *Appl. Phys. Lett.* **2004**, *85*, 3854−3856.
(59) McDaniel, A. A.; Hsu, J. W. P.; Gabor, A. M. Near-Field Scanning Optical Microscopy studies of $Cu(In,Ga)Se_2$ Solar Cells. *Appl. Phys. Lett.* **1997**, *70*, 3555−3557.
(60) Bao, W.; Melli, M.; Caselli, N.; Riboli, F.; Wiersma, D. S.; Staffaroni, M.; Choo, H.; Ogletree, D. F.; Aloni, S.; Bokor, J.; et al. Mapping Local Charge Recombination Heterogeneity by Multidimensional Nanospectroscopic Imaging. *Science* **2012**, *338*, 1317−21.
(61) Haegel, N. M. Integrating Electron and Near-Field Optics: Dual Vision for the Nanoworld. *Nanophotonics* **2014**, *3*, 75−89.
(62) Shirakata, S.; Nakada, T. Time-Resolved Photoluminescence in $Cu(In,Ga)Se_2$ Thin Films and Solar Cells. *Thin Solid Films* **2007**, *515*, 6151−6154.
(63) Todorov, T. K.; Tang, J.; Bag, S.; Gunawan, O.; Gokmen, T.; Zhu, Y.; Mitzi, D. B. Beyond 11% Efficiency: Characteristics of State-of-the-Art $Cu_2ZnSn(S,Se)_4$ Solar Cells. *Adv. Energy Mater.* **2013**, *3*, 34−38.
(64) D'Innocenzo, V.; Srimath Kandada, A. R.; De Bastiani, M.; Gandini, M.; Petrozza, A. Tuning the Light Emission Properties by Band Gap Engineering in Hybrid Lead Halide Perovskite. *J. Am. Chem. Soc.* **2014**, *136*, 17730−17733.
(65) deQuilettes, D. W.; Koch, S.; Burke, S.; Paranji, R. K.; Shropshire, A. J.; Ziffer, M. E.; Ginger, D. S. Photoluminescence Lifetimes Exceeding 8 μs and Quantum Yields Exceeding 30% in Hybrid Perovskite Thin Films by Ligand Passivation. *ACS Energy Lett.* **2016**, *1*, 438−444.
(66) Barnard, E. S.; Hoke, E. T.; Connor, S. T.; Groves, J. R.; Kuykendall, T.; Yan, Z.; Samulon, E. C.; Bourret-Courchesne, E. D.; Aloni, S.; Schuck, P. J.; et al. Probing Carrier Lifetimes in Photovoltaic Materials Using Subsurface Two-Photon Microscopy. *Sci. Rep.* **2013**, *3*, 2098.
(67) Chen, W.; Wen, X.; Latzel, M.; Heilmann, M.; Yang, J.; Dai, X.; Huang, S.; Shrestha, S.; Patterson, R.; Christiansen, S.; et al. Nanoscale Characterization of Carrier Dynamic and Surface Passivation in InGaN/GaN Multiple Quantum Wells on GaN Nanorods. *ACS Appl. Mater. Interfaces* **2016**, *8*, 31887−31893.
(68) Richter, A.; Behme, G.; Süptitz, M.; Lienau, C.; Elsaesser, T.; Ramsteiner, M.; Nötzel, R.; Ploog, K. H. Real-Space Transfer and Trapping of Carriers into Single GaAs Quantum Wires Studied by Near-Field Optical Spectroscopy. *Phys. Rev. Lett.* **1997**, *79*, 2145−2148.
(69) Saliba, M.; Matsui, T.; Seo, J.-Y.; Domanski, K.; Correa-Baena, J.-P.; Nazeeruddin, M. K.; Zakeeruddin, S. M.; Tress, W.; Abate, A.; Hagfeldt, A.; et al. Cesium-Containing Triple Cation Perovskite Solar Cells: Improved Stability, Reproducibility and High Efficiency. *Energy Environ. Sci.* **2016**, *9*, 1989−1997.
(70) Leblebici, S. Y.; Leppert, L.; Li, Y.; Reyes-Lillo, S. E.; Wickenburg, S.; Wong, E.; Lee, J.; Melli, M.; Ziegler, D.; Angell, D. K.; et al. Facet-Dependent Photovoltaic Efficiency Variations in Single Grains of Hybrid Halide Perovskite. *Nat. Energy* **2016**, *1*, 16093.
(71) Bergmann, V. W.; Weber, S. A. L.; Javier Ramos, F.; Nazeeruddin, M. K.; Grätzel, M.; Li, D.; Domanski, A. L.; Lieberwirth, I.; Ahmad, S.; Berger, R. Real-Space Observation of Unbalanced Charge Distribution Inside a Perovskite-Sensitized Solar Cell. *Nat. Commun.* **2014**, *5*, 5001.
(72) Chakraborty, S.; Xie, W.; Mathews, N.; Sherburne, M.; Ahuja, R.; Asta, M.; Mhaisalkar, S. G. Rational Design: A High-Throughput Computational Screening and Experimental Validation Methodology for Lead-Free and Emergent Hybrid Perovskites. *ACS Energy Lett.* **2017**, *2*, 837−845.
(73) Shi, Z.; Guo, J.; Chen, Y.; Li, Q.; Pan, Y.; Zhang, H.; Xia, Y.; Huang, W. Lead-Free Organic−Inorganic Hybrid Perovskites for Photovoltaic Applications: Recent Advances and Perspectives. *Adv. Mater.* **2017**, *29*, 1605005.
(74) Duong, T.; Wu, Y.; Shen, H.; Peng, J.; Fu, X.; Jacobs, D.; Wang, E.-C.; Kho, T. C.; Fong, K. C.; Stocks, M.; et al. Rubidium Multication Perovskite with Optimized Bandgap for Perovskite-Silicon Tandem with over 26% Efficiency. *Adv. Energy Mater.* **2017**, 1700228.
(75) Kalinin, S. V.; Sumpter, B. G.; Archibald, R. K. Big-Deep-Smart Data in Imaging for Guiding Materials Design. *Nat. Mater.* **2015**, *14*, 973−980.
(76) Strelcov, E.; Belianinov, A.; Hsieh, Y.-H.; Jesse, S.; Baddorf, A. P.; Chu, Y.-H.; Kalinin, S. V. Deep Data Analysis of Conductive Phenomena on Complex Oxide Interfaces: Physics from Data Mining. *ACS Nano* **2014**, *8*, 6449−6457.
(77) Jesse, S.; Kalinin, S. V. Principal Component and Spatial Correlation Analysis of Spectroscopic-Imaging Data in Scanning Probe Microscopy. *Nanotechnology* **2009**, *20*, 085714.

NOTE ADDED AFTER ASAP PUBLICATION

This paper was published ASAP on June 24, 2017 with an error in Figure 3. The corrected paper was reposted on July 27, 2017.

DOI: 10.1021/acsenergylett.7b00382
ACS Energy Lett. 2017, 2, 1825−1834